

Accepted Manuscript

Removal of several pesticides in a falling water film DBD reactor with activated carbon textile: Energy efficiency

Patrick Vanraes, Houria Ghodbane, Dries Davister, Niels Wardenier, Anton Nikiforov, Yannick P. Verheust, Stijn W.H. Van Hulle, Oualid Hamdaoui, Jeroen Vandamme, Jim Van Durme, Pieter Surmont, Frederic Lynen, Christophe Leys

PII: S0043-1354(17)30171-9

DOI: [10.1016/j.watres.2017.03.004](https://doi.org/10.1016/j.watres.2017.03.004)

Reference: WR 12741

To appear in: *Water Research*

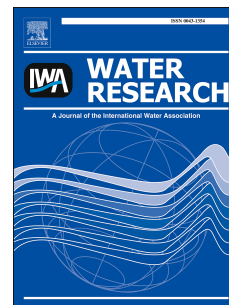
Received Date: 5 December 2016

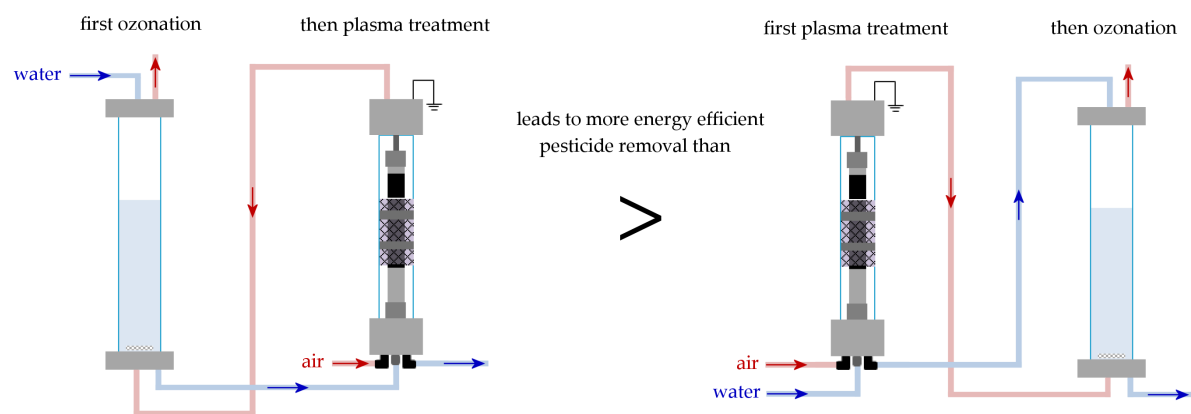
Revised Date: 27 February 2017

Accepted Date: 4 March 2017

Please cite this article as: Vanraes, P., Ghodbane, H., Davister, D., Wardenier, N., Nikiforov, A., Verheust, Y.P., Van Hulle, S.W.H., Hamdaoui, O., Vandamme, J., Van Durme, J., Surmont, P., Lynen, F., Leys, C., Removal of several pesticides in a falling water film DBD reactor with activated carbon textile: Energy efficiency, *Water Research* (2017), doi: 10.1016/j.watres.2017.03.004.

This is a PDF file of an unedited manuscript that has been accepted for publication. As a service to our customers we are providing this early version of the manuscript. The manuscript will undergo copyediting, typesetting, and review of the resulting proof before it is published in its final form. Please note that during the production process errors may be discovered which could affect the content, and all legal disclaimers that apply to the journal pertain.





ACCEPTED MANUSCRIPT

26 **Abstract**

27 Bio-recalcitrant micropollutants are often insufficiently removed by modern
28 wastewater treatment plants to meet the future demands worldwide. Therefore,
29 several advanced oxidation techniques, including cold plasma technology, are being
30 investigated as effective complementary water treatment methods. In order to permit
31 industrial implementation, energy demand of these techniques needs to be
32 minimized. To this end, we have developed an electrical discharge reactor where
33 water treatment by dielectric barrier discharge (DBD) is combined with adsorption
34 on activated carbon textile and additional ozonation. The reactor consists of a DBD
35 plasma chamber, including the adsorptive textile, and an ozonation chamber, where
36 the DBD generated plasma gas is bubbled. In the present paper, this reactor is further
37 characterized and optimized in terms of its energy efficiency for removal of the five
38 pesticides α -HCH, pentachlorobenzene, alachlor, diuron and isoproturon, with initial
39 concentrations ranging between 22 and 430 $\mu\text{g/L}$. Energy efficiency of the reactor is
40 found to increase significantly when initial micropollutant concentration is
41 decreased, when duty cycle is decreased and when oxygen is used as feed gas as
42 compared to air and argon. Overall reactor performance is improved as well by
43 making it work in single-pass operation, where water is flowing through the system
44 only once. The results are explained with insights found in literature and practical
45 implications are discussed. For the used operational conditions and settings, α -HCH
46 is the most persistent pesticide in the reactor, with a minimal achieved electrical
47 energy per order of 8 kWh/m^3 , while a most efficient removal of 3 kWh/m^3 or lower
48 was reached for the four other pesticides.

49

50

51 *Keywords:* plasma treatment; pesticides; energy yield; nitrite; nitrate; peroxone

52

53 **1. Introduction**

54 With ongoing improvement of chemical analytical methods, various
55 compounds and their transformation products are increasingly
56 detected in water bodies in low concentrations in the range of
57 microgram to nanogram per liter. Among these so-called
58 micropollutants are food additives, industrial chemicals, pesticides,
59 pharmaceuticals and personal care products. Despite their low
60 concentrations, various hazardous environmental effects have been
61 observed (Milla et al. 2011, Rizzo et al. 2013). Additionally, there is
62 growing concern about their effect on human health. Conventional
63 wastewater treatment plants are often unable to sufficiently remove
64 these micropollutants (Luo et al. 2014). Preventive measures are,
65 unfortunately, strongly limited by the increasing demand, while
66 enhancement of conventional techniques often has negligible effect
67 on many persistent micropollutants (Luo et al. 2014). Therefore,
68 advanced treatment methods, such as activated carbon, have recently
69 received more attention for their effective removal of
70 micropollutants. Nonetheless, these techniques are associated with
71 high costs and the additional problem of hazardous concentrate or
72 adsorbate disposal. As a promising alternative, advanced oxidation
73 techniques are the most effective available methods to decompose
74 bio-recalcitrant organics. Since their energy costs are high up to now,
75 research needs to focus on optimization of their energy efficiency.
76 Combination of oxidation methods with each other or with other
77 advanced treatment techniques is hereto proposed in many reviews as
78 an effective strategy (Ghatak 2014, Oturan and Aaron 2014).

79

80 Amongst the advanced oxidation techniques, plasma technology for
81 water treatment takes an interesting place, since it is able to produce a
82 wide spectrum of oxidative species, leading to a low selectivity of the
83 decomposition process. Moreover, its flexible design facilitates
84 synergetic combination with other advanced separation and oxidation
85 methods. In prior research, we have found a synergy between
86 micropollutant adsorption and dielectric barrier discharge (Vanraes et
87 al. 2015a). Further, we have developed and characterized a new type
88 of plasma reactor for water treatment (Vanraes et al. 2015b). In this
89 reactor, micropollutant decomposition by atmospheric dielectric
90 barrier discharge in dry air is combined with adsorption on activated
91 carbon textile and with extra bubbling of plasma-generated ozone. To
92 this end, the water solution under treatment is recirculated between a
93 plasma chamber with the carbon textile and an ozonation chamber.
94 Atrazine was used as model micropollutant with an initial
95 concentration of 30 µg/L. Plasma gas bubbling contributed to up to
96 40.5% of total atrazine decomposition, confirming an interesting
97 optimization of the reactor's energy efficiency, as compared to
98 plasma treatment alone.

99

100 In the present study, our reactor is investigated and optimized further
101 in terms of its energy efficiency. For this purpose, five persistent
102 pesticides with significantly diverse properties are investigated for
103 their removal kinetics: α -hexachlorocyclohexane (α -HCH),
104 pentachlorobenzene (PeCB), alachlor, diuron and isoproturon. Their
105 variety permits to gain a more comprehensive view on the overall
106 reactor performance and optimization. As in our previous research,

107 initial concentration of the pollutants is taken in the order of 100
108 $\mu\text{g/L}$, to have sufficient agreement with real-world situations and
109 with the maximally allowed limits defined by the United States
110 Environmental Protection Agency (EPA 2007), by the World Health
111 Organization (WHO 2008) and by the European Parliament and the
112 Council (EC 2006). Prior to micropollutant removal kinetics analysis,
113 the evolution of pH and conductivity during plasma treatment is
114 investigated and explained. Next, the contribution of micropollutant
115 evaporation and adsorption to the total removal process is studied in
116 detail. Afterwards, the effect of pH, salt addition, initial
117 concentration, applied power and feed gas on the reactor's
118 performance is shown and compared with insights from literature.
119 Finally, the reactor is modified to work in single-pass operation,
120 where water is flowing through the system only once. The influence
121 of the sequence of plasma chamber and ozonation chamber is
122 discussed and the reactor's performance is compared with its
123 recirculated batch operation.

124 **2. Experimental methods and materials**

125 *2.1. DBD water treatment reactor and determination of solution* 126 *parameters*

127 Each pesticide removal experiment is performed with the plasma
128 reactor described in our previous study (Vanraes et al. 2015b). In
129 short, a pesticide solution is continuously recirculated between a
130 plasma chamber and an ozonation chamber. Based on the water flow
131 rate of 95.3 mL/min and solution volume of 400 mL in the ozonation
132 chamber, hydraulic residence time in the ozonation chamber is

133 calculated to be 4.20 min. Relative to this value, hydraulic residence
134 time in the plasma chamber is negligible (0.86 ± 0.02 s). The plasma
135 chamber consists of a coaxial DBD electrode system, where the
136 grounded inner electrode is covered with one layer of Zorflex®,
137 100% activated carbon textile. The solution under treatment flows
138 downwards along the carbon textile. Plasma is generated in dry air
139 over the carbon textile by applying a pulsed AC high voltage on the
140 outer mesh electrode that covers the tubular quartz glass dielectric
141 barrier. The duty cycle of the power is defined as the fraction of time
142 during which the plasma is operating, given by the ratio of the
143 variable power pulse width to the fixed pulse period of 30 ms. In the
144 ozonation chamber, the ozone generated in the plasma chamber is
145 bubbled through the solution for additional pesticide oxidation, in
146 order to enhance the reactor efficiency without extra energy input.
147 Solution samples for micropollutant analysis are taken after passing
148 the ozonation chamber. The reactor standard settings are different
149 from the ones used in previous work and are given in Table 1.
150 Information on the Zorflex® textile, on the method for power
151 determination and on the measurement methods of pH and
152 conductivity is given in (Vanraes et al. 2015b). The structural
153 formulas of all compounds are depicted in Figure 1 and their most
154 relevant physical and chemical properties are enlisted in Table A.1 in
155 the Appendix. Initial solution of each micropollutant was made by
156 dissolving a concentration C_0 (see Table 2) of the pesticide in
157 deionized water. Unless mentioned otherwise, no salt addition was
158 used.
159

160 2.2. *Micropollutant concentration measurement method.*

161 Alachlor and diuron concentration is measured by means of an
162 Agilent GC-MS (HP 6890 Series GC System, 5973 Mass Selective
163 Detector) equipped with a cross-linked methyl silicone column (ZB-
164 5MS, 30 m x 0.25 mm, 0.25 μm film thickness; Phenomenex).
165 Before extraction, 19.00 g of the solution was hermetically sealed in
166 20 mL vials, where alachlor was incubated for 5 minutes at 50 °C
167 and diuron for 1 minute at 30 °C using agitation. Extraction of both
168 dissolved compounds was performed with a MPS-2 XYZ
169 autosampler equipped with a headspace-solid phase microextraction
170 unit (multi-PurposeSampler® or MPS®, Gerstel®, Mülheim and der
171 Ruhr, Germany). Extraction from the water matrix occurred on a
172 SPME fibre (75 μm Carboxen/Polydimethylsiloxane (CAR/PDMS),
173 fused silica fibre core, Supelco, USA), for 45 minutes at 50°C in the
174 case of alachlor and for 30 minutes at 30°C in the case for diuron.
175 The compounds were separated using Helium as the carrier gas (flow
176 rate 1 mL min⁻¹). For alachlor, the temperature gradient was 60 °C
177 (6 min) to 160 °C at 15 °C min⁻¹, held 11 minutes; then 7 °C/min to
178 205 °C for 0 min; then 25 °C/min to 250 °C for 5 min. For diuron,
179 the gradient was 35 °C (6 min) to 160 °C at 15 °C min⁻¹, held 5
180 minutes; then 100 °C/min to 250 °C for 1 min. The injector and
181 transfer lines were maintained isothermally at 250 °C and 280 °C,
182 respectively. Both compounds are measured in Selected Ion Mode
183 (SIM), alachlor at a retention time of 28.4 min and diuron at 16.3
184 min. Calibration of the detector was made with solutions of known
185 concentration, from 1 to 100 $\mu\text{g/L}$. The integrated peak area in the
186 obtained chromatogram was found to be linear with concentration in

187 this range for each micropollutant.
188
189 Analysis of α -HCH, PeCB and isoproturon was carried out with
190 Agilent GC-MS (6890 series GC system, 5973 MS) using
191 Chemstation software. Before analysis, 20 mL water samples were
192 extracted towards CH_2Cl_2 solvent by means of liquid-liquid
193 extraction. α -HCH and PeCB extraction was executed with addition
194 of 2 mL of CH_2Cl_2 . The method was improved for isoproturon by
195 using a CH_2Cl_2 volume of only 1 mL. The samples were shaken by
196 hand for 5 min in 22.5 mL sized vials. Afterwards, 0.6 mL of the
197 CH_2Cl_2 drop was separated by means of a micropipette. In the case of
198 α -HCH and PeCB, 2 grains of dry CaCl_2 were added in order to
199 absorb any water traces in the sample. Splitless injection of 1 μL
200 sample occurred at temperature of 250°C and pressure of 78.4 kPa in
201 HP-5 MS column (0.25 mm x 30 m x 0.25 μm) with constant He
202 flow of 1 mL/min. α -HCH and PeCB were measured with an
203 identical oven program. Oven temperature started at 125 °C, rising to
204 195 °C at 25 °C/min and further rising to 210 °C at 10 °C/min with a
205 final hold of 1.5 min. Mass spectra were recorded in SIM mode with
206 target ion 219 and qualifier ions 181 and 183 in the case of α -HCH
207 and with target ion 250 and qualifier ions 247 and 252 in the case of
208 PeCB (MS source at 230°C, MS quad at 150 °C, solvent delay of 2
209 min). For isoproturon, splitless injection of 1 μL sample occurred at
210 temperature of 270°C and pressure of 68.1 kPa. Oven temperature
211 started at 90 °C held for 1 min, rising to 190 °C at 40 °C/min and
212 further rising to 270 °C at 20 °C/min with a final hold of 2 min. Mass
213 spectra were recorded in SIM mode with target ion 146 and qualifier

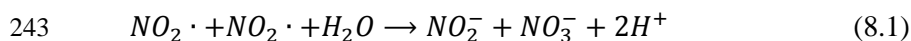
ions 161 and 128 (solvent delay of 3 min). All other instrumental settings were kept the same. Peaks of α -HCH, PeCB and isoproturon were detected at a retention time of 5.13 min, 4.03 min and 4.06 min, respectively. All three compounds were calibrated for the range of 0 to 1000 $\mu\text{g/L}$, where linear dependence on concentration was found. Naphthalene was used as internal standard.

3. Results and discussion

3.1. Conductivity and pH

The formation of aqueous radicals and other species by plasma treatment induces a change in conductivity and pH during each experiment. Figure 2a gives an example of both solution parameters as a function of treatment time, where the initial conductivity of 350 $\mu\text{S/cm}$ was prepared by addition of $\text{NaH}_2\text{PO}_4 \cdot 2\text{H}_2\text{O}$ to demineralized water. As can be seen, conductivity grows gradually towards approximately 1.3 mS/cm during 30 min, while pH drops abruptly towards a value around 3 in the first 2.5 min of treatment time, followed by a slight further decrease. The end values of conductivity and pH after 30 min were found to be rather independent of initial conductivity and pH. When the solution is only recirculated through the ozonation chamber, hence without direct contact to the active plasma region, the sharp pH drop at the start of the experiment does not occur, as shown in Figure 2b. The latter experiment is performed by recirculating a separate 500 mL solution of deionized water through the plasma chamber. This difference is explained with the formation of aqueous nitrites and nitrates in the plasma chamber through the dissolution of nitrogen oxides formed in the plasma by

240 reactions of dissociated N₂ and O₂. During this process, H⁺ ions are
241 generated in the water phase, as described with the overall reactions
242 (Lukes et al. 2014):



245 Other species can contribute to pH and conductivity change as well,
246 including O₃ and H₂O₂. Figures 2c-d show the end values of both
247 solution parameters for different power settings, where duty cycle is
248 varied. It was found that power variation at fixed duty cycle has a
249 very limited effect on the final pH value. Increasing the duty cycle,
250 on the other hand, has a stronger effect, causing a reduction of the
251 end pH, due to more abundant formation of nitrites and nitrates.
252 Accordingly, end conductivity is influenced stronger by duty cycle
253 than by power at fixed duty cycle and is linearly proportional to both.
254

255 *3.2. Kinetic analysis for removal of 5 micropollutants*

256 In this section, the reactor's performance is investigated in detail as a
257 function of operational parameters and working conditions. To this
258 end, removal experiments are performed in parallel for 5 selected
259 micropollutants with diverse properties (see Table A.1), to gain a
260 comprehensive view and to uncover compound-related issues, if any.
261 More statistical information of these experiments is found in Table
262 B.1 in the Appendix.

263

264 Figure 3 shows the removal of each micropollutant under the
265 standard conditions of Table 1 in air atmosphere for the three

266 situations (i) with plasma generation, (ii) without plasma generation
267 but with Zorflex® and air bubbling and (iii) without plasma
268 generation in absence of Zorflex®, but with air bubbling. The
269 corresponding nonlinear least squares exponential fitting is found by
270 means of the Levenberg-Marquardt algorithm. Table 2 enlists the
271 reciprocal time constant τ^{-1} or pseudo-first-order reaction rate
272 constant k for each removal experiment, as deduced from the fitting,
273 as well as the initial concentration of each micropollutant. As
274 expected, the most volatile compounds, α -HCH and PeCB, decline
275 fastest by air bubbling alone, while the most involatile compound,
276 isoproturon, does not evaporate at all. Surprisingly, evaporation of
277 diuron is relatively high. This is possibly due to an inaccuracy in the
278 reported Henry law constant H of diuron, as this value is solely based
279 on calculations (Giacomazzi and Cochet 2004) and no experimental
280 confirmation was found in literature. Apart from this deviation, the
281 observed order of volatility $\text{PeCB} > \alpha\text{-HCH} > \text{diuron} > \text{alachlor} >$
282 isoproturon in our experiments agrees well with the literature values
283 of the Henry law constant.

284

285 When Zorflex® is added in the reactor, stronger removal is observed
286 for all micropollutants. Alachlor and isoproturon appear to be the
287 most efficiently removed compounds by adsorption, followed by
288 diuron. PeCB, on the other hand, is adsorbed least efficiently in
289 addition to evaporation. With the assumption that evaporation and
290 adsorption have an accumulative effect, these observations can be
291 explained as follows. According to Moreno-Castilla, four features of
292 an organic compound regulate its rate of adsorption on activated

293 carbon (Moreno-Castilla 2004):

- 294 1. molecular size;
- 295 2. acid dissociation constant pKa, in case it is an electrolyte;
- 296 3. solubility;
- 297 4. nature of substituents, in case it is aromatic.

298 The molecular size determines the compound's accessibility to the
299 micro-pores of the carbon. The pKa value controls the dissociation of
300 an electrolytic compound into ions, dependent on solution pH.
301 Consequently, adsorption of the resulting organic ion is strongly
302 regulated by electrostatic interaction with the charges on the carbon
303 surface. Since all selected micropollutants in our study are similar in
304 size and nonionic, differences in their adsorption rate are supposed to
305 be regulated predominantly by other factors, such as their solubility
306 and their substituents. Each molecule's water solubility (see Table
307 A.1 in the Appendix) is directly related to its hydrophobicity, which
308 dictates how easily it is rejected by the aqueous solution and thus
309 how readily it is accepted by another phase contacting the solution.
310 Clearly, solubility is not the dominant factor, since the best soluble
311 compounds, alachlor and isoproturon, are adsorbed more rapidly,
312 while the most hydrophobic molecules, α -HCH and PeCB, are
313 adsorbed worst. The amount of electron-withdrawing chlorine atoms
314 on the aromatic ring of a micropollutant, on the other hand, seems to
315 strongly regulate the adsorption rate. Namely, electron-withdrawing
316 or electron-donating substituents on the aromatic ring are expected to
317 affect the π - π dispersion interaction between the aromatic ring of the
318 compound and the aromatic structure of the graphene layers
319 (Moreno-Castilla 2004). Possibly, donor-acceptor interactions

320 between the compound's aromatic ring or substituents and functional
321 surface groups such as carbonyl can also play a role. The five
322 chlorine atoms present in PeCB strongly decrease the electron
323 density in the ring, which explains its low adsorption on Zorflex®.
324 Alachlor and isoproturon, in contrast, have an electron-rich aromatic
325 cycle because of the absence of direct chlorine substitution. Diuron
326 has a very similar molecular structure to isoproturon, but with two
327 chlorines attached to the ring, corresponding to a lower adsorption
328 rate. This is in good agreement with the observed results, suggesting
329 that the above mentioned π - π dispersion or acceptor-donor
330 interactions are the dominant mechanisms for adsorption in our
331 experiments.

332

333 When plasma is turned on, all micropollutants are removed to higher
334 extent. The additional removal process by plasma oxidation is
335 strongest for isoproturon, diuron and alachlor, while α -HCH and
336 PeCB appear most recalcitrant to oxidation by plasma-generated
337 aqueous oxidants. It should be emphasized, nonetheless, that
338 decomposition processes occur in the vapor phase as well, under
339 influence of gaseous oxidants. A detailed study on this topic is made
340 by Ognier et al., who used an AC powered coaxial DBD reactor
341 similar to ours but without additional bubbling for treatment of 4
342 volatile compounds: acetic acid, phenol, ethanol and 1-heptanol
343 (Ognier et al. 2009). When plasma was switched on in their reactor,
344 an increase was observed in mass transfer of each pollutant from the
345 liquid to the gas phase, proportional to the corresponding Henry law
346 constant. This mass transfer increased was attributed to the intense

347 mixing in the liquid film and the reaction of the pollutant with active
 348 species in the gaseous phase, in agreement with computational fluid
 349 dynamic modelling results. The same authors also measured a
 350 minimum of 95 % decomposition of these compounds in the gas
 351 phase. Accordingly, decomposition in the gas phase was found to be
 352 significantly more effective than decomposition in the liquid phase.

353

354 Energy efficiency of plasma reactors is often expressed by the energy
 355 yield G_{50} (in g/kWh) for 50% pesticide removal, which is calculated
 356 by adapting the formula from (Hijosa-Valseiro et al. 2013),

$$357 \quad G_{50} = -A \frac{kC_0V}{2P \ln(0.5)} \quad (8.3)$$

358 where $A = 3.6 \times 10^6$ J/kWh is a unit conversion factor, k is reaction
 359 rate constant (in s^{-1}), C_0 is initial concentration (in g/L), V is treated
 360 water volume (in L) and P is applied power (in W). G_{50} is, however,
 361 not recommended as comparative parameter for reactor energy
 362 efficiency, since it strongly depends on initial pollutant concentration
 363 C_0 . Therefore, we used electrical energy per order EEO, defined as
 364 the number of kilowatt hours of electrical energy required to reduce a
 365 pollutant's concentration by 1 order of magnitude (90%) in 1 m^3 of
 366 contaminated water (Wohlers et al. 2009),

$$367 \quad EEO = \frac{\ln(10) \times P}{3600 \times V \times k} \quad (8.4)$$

368 Table 2 gives the energy yield G_{50} and electrical energy per order
 369 EEO of the overall removal for each micropollutant in our reactor.

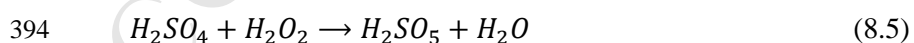
370 The input energy required for 90% reduction increases in the order:
 371 diuron < isoproturon < alachlor < PeCB < α -HCH. With the used
 372 reactor settings, it takes about 7 times as much energy to remove the
 373 same amount of α -HCH from the solution as compared to diuron,

374 indicating that EEO values in our reactor for different compounds
375 can vary over almost one order of magnitude. With the inclusion of
376 more micropollutants, this range is likely to expand further. As
377 should be noted, the contribution of the oxidation by-products to the
378 overall micropollutant concentration in our reactor is expected to be
379 negligible, based on HPLC-TOF-MS analysis. More detailed
380 information on the by-product analysis will be published in a
381 separate paper.

382

383 *3.2.1. Effect of pH and salt addition*

384 As this work mainly focuses on reactor characterization and
385 optimization, the influence of the water matrix is illustrated only for
386 isoproturon. Figure C.1a in the Appendix shows the decomposition
387 of the pesticide for different initial pH. In the standard experiment
388 mentioned above, the initial pH was 5.03. Reduction of pH to 4.2
389 with addition of H₂SO₄ has little effect on the oxidation rate, but
390 further decrease to 2.08 leads to significant improvement of the
391 degradation process. This is possibly due to the formation of
392 peroxymonosulfuric acid (H₂SO₅), also known as Caro's acid, via the
393 reaction (McDonogh and Sanders 1995)

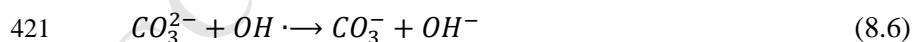


395 Peroxymonosulfuric acid is one of the strongest oxidants, which is
396 able to decompose organics non-selectively with a redox potential
397 comparable to the one of the hydroxyl radical (Spivey et al. 2015).
398 As an additional explanation, the lower pH leads to higher H₂O₂
399 stability, which can cause stronger isoproturon decomposition.
400 Increase of the pH to 7.2 with addition of NaOH quenches the

401 oxidation of isotroturon, while further increase to a pH of 10
402 enhances the decomposition process again. Since isotroturon is
403 relatively reactive to ozone, with reported values of k_{O_3} from 141 to
404 $2191 \text{ M}^{-1} \text{ s}^{-1}$ (Table A.1), its degradation in our reactor is strongly
405 influenced by the stability of aqueous O_3 . Elevation of pH is known
406 to gradually lower the stability of ozone, explaining the initial
407 decrease. It is, however, less known that in highly alkaline solution,
408 starting from addition of 5 M NaOH, ozone stability abruptly rises
409 again (Eriksson 2005, Heidt and Landi 1967). In the case that this
410 stage of high O_3 stability has not been reached yet at $\text{pH} = 10$, the re-
411 established decomposition rate can alternatively be explained with
412 the peroxone process. Namely, the peroxone rate constant increases
413 with pH and can take the upper hand in isotroturon decomposition
414 above a certain pH value (Catalkaya and Kargi 2009).

415

416 The influence of salt addition is shown in Figure C.1b. In the
417 accuracy of the measurements, addition of NaH_2PO_4 and Na_2SO_4 did
418 not have any visible effect on isotroturon decomposition. NaHCO_3 ,
419 however, significantly lowered the oxidation rate. Carbonate is an
420 effective OH scavenger through the reaction (Eriksson 2005):



422 Therefore, the reduction in the reaction rate is due to inhibition of
423 OH radical attack. As the above results indicate, direct attack by OH
424 radicals plays a significant role during the degradation of isotroturon
425 at the standard conditions.

426

427 3.2.2. *Effect of initial concentration*

428 EEO is a comparative parameter of preference for reactor energy
429 efficiency in organic removal. A priori, it is more advisable to carry
430 out such comparison for a fixed initial pollutant concentration C_0 , to
431 exclude any concentration related effects. In practice, however, it is
432 useful to experimentally investigate the influence of the initial
433 pollutant concentration on its removal rate and thus on the EEO
434 value. As shown in Figure C.2 and Table C.1 in the Appendix, this
435 influence is relatively small for our reactor. With decreasing C_0 , a
436 drop in EEO is observed for α -HCH, alachlor, diuron and
437 isoproturon. This is in good agreement with the observation of many
438 other authors. Table A.2 in the Appendix enlists all reported effects
439 of a decreasing initial concentration of a water pollutant on its
440 decomposition rate constant that have been found in literature on
441 plasma reactors. For 25 cases dealing with different reactor types,
442 decreasing C_0 caused an increase in decomposition rate. Frequently,
443 authors explain this concentration effect with a decrease in
444 competition for OH radicals between the pollutant molecules as well
445 as their by-products, assuming a constant concentration of OH
446 radicals or other dominant oxidants. With the introduction of EEO as
447 a physical quantity for energy efficiency, Cater et al. already stated
448 this for advanced oxidation processes in general (Cater et al. 2000),
449 as shortly reviewed for pharmaceutical compounds in (Magureanu et
450 al. 2010). The magnitude for this effect is, however, extremer for
451 higher concentrations, while the concentration effect can become
452 negligible for lower concentrations. A nearly constant decomposition
453 rate has for instance been observed for the lower concentration

454 ranges of 0.1 to 0.3 mg/L 17 β -Estradiol in DBD over water in (Gao
455 et al. 2013), 1.9 to 3.3 mg/L rhodamine B in the DBD spray reactor
456 of (Nakagawa et al. 2003), 5 to 10 mg/L acid blue 25 treated by DC
457 glow discharge (Ghodbane et al. 2014) and 5 to 10 mg/L paraquat
458 under gliding arc (Fouodjouo et al. 2013). This explains the relatively
459 small deviations in our experiments. Accordingly, the strongest
460 relative change of the oxidation rate and thus of EEO is observed for
461 α -HCH, the compound with highest initial concentration (see Table
462 C.1).

463

464 The above results and discussion imply that, generally, literature
465 values of the oxidation rate constant for micropollutants in plasma
466 reactors are underestimations for realistic situations in urban and
467 rural wastewater treatment plants, where concentrations up to a few
468 microgram per liter are usually measured. Even in hospital
469 wastewater, concentrations are in general only one order of
470 magnitude higher (Verlicchi et al. 2010). Therefore, we want to
471 accentuate the importance of experimental research with realistic or
472 sufficiently low micropollutant concentrations as in the present work,
473 in order to gather energy efficiency data that is more representative
474 for real-world applications. It should be taken into account, however,
475 that the raw wastewater's matrix will influence the aqueous oxidative
476 chemistry, likely increasing the total energy demand.

477

478 ***3.2.3. Effect of power at constant duty cycle***

479 Applied power in our reactor can be changed in two ways: by varying
480 the momentary power and by adjusting the duty cycle. The duty cycle

481 DC of the power source is defined as the fraction of time in which the
482 power is active. Figure C.3 and Table C.2 in the Appendix present
483 the results for variation of the momentary power at a fixed duty cycle
484 DC = 0.15. As expected, increasing power leads in general to a
485 higher oxidation rate, in agreement with other DBD reactors (see
486 Table A.3 in the Appendix). For α -HCH, PeCB and isoproturon, G_{50}
487 drops and EEO rises slightly for higher power. For alachlor, energy
488 efficiency remains constant in the accuracy of the measurements, as
489 in the case of atrazine reported in our previous research (Vanraes et
490 al. 2015b). For diuron, there is a slight rise in energy efficiency when
491 power is increased. Table A.3 shows energy efficiency data as a
492 function of applied power for four AC powered DBD reactors with
493 discharge in air. Since the operational conditions of these reactors,
494 including input power, are similar to our experiments, this data is
495 expected to be representative for our study. G_{50} and EEO are
496 calculated from the reported values of the reaction rate constant,
497 power, initial concentration and solution volume. According to these
498 data, there is no consistent trend of energy efficiency as a function of
499 applied power. Since the four compounds in Table A.3 are
500 decomposed in very similar reactors, these results suggest that the
501 effect of power might be specific for each compound. In our reactor,
502 the influence of adsorption on Zorflex® is compound-specific and
503 should be considered as well. In any case, the dependency of EEO on
504 power seems to be rather limited, which is beneficial for applications
505 where removal rate needs to be controlled as a function of the
506 influent micropollutant concentrations.

507

508 **3.2.4. Effect of duty cycle**

509 Figure 4 and Table C.3 in the Appendix present the effect of duty
510 cycle on compound removal in our reactor. As seen from the
511 measured data, an increase in duty cycle leads to a higher oxidation
512 rate in general, except for diuron, for which removal rate remains
513 constant in the accuracy of the measurement. Nonetheless, a higher
514 duty cycle results in a significant decrease in energy efficiency. The
515 same effect has been found with the gas phase DBD reactor of
516 (Olszewski et al. 2014) with pulse-modulated AC power, where
517 increasing the duty cycle from 25% to 100% lowered energy
518 efficiency 2.11 times. The authors explained the latter effect with
519 additional organic degradation during plasma off time under
520 influence of long living reactive species such as O_3 and H_2O_2 . As
521 seen in section 3.1, a higher duty cycle results in a lower pH due to
522 stronger NO_2^- and NO_3^- formation. These anions and their conjugated
523 acids can inhibit oxidation by O_3 and OH , which gives an alternative
524 explanation for the reduction in energy efficiency at higher duty
525 cycle. This effect will be discussed in more detail in section 3.2.6.
526 The effect of duty cycle on the pollutant removal can also be
527 explained with significant gas temperature increase in the plasma
528 zone, which inhibits O_3 and H_2O_2 production.

529

530 **3.2.5. Effect of feed gas**

531 The removal of each micropollutant under air, argon and oxygen
532 plasma is compared in Figure 5 and Table 3. Dry gases are used, but
533 significant vapor presence is expected in the plasma chamber due to
534 evaporation. Reactor performance is significantly enhanced with

535 oxygen, except for α -HCH. Unfortunately, no data is available on the
536 reaction rate constants k_{O_3} and k_{OH} of α -HCH with ozone and OH
537 radicals, respectively. However, the isomer γ -HCH is known to be
538 very resistant to ozonation with $k_{O_3} < 0.04 \text{ M}^{-1} \text{ s}^{-1}$ (Roche and Prados
539 1995, Yao and Haag 1991), while it is oxidized with OH radicals
540 with reaction rate $k_{OH} = 7.5 \times 10^8 \text{ M}^{-1} \text{ s}^{-1}$ (Haag and Yao 1992).
541 According to Camel and Bermond, pesticides containing several
542 chlorine atoms without unsaturated bonds, such as α -HCH and γ -
543 HCH, are generally unreactive to ozone, while presence of accessible
544 unsaturated cycles as in PeCB leads to higher reactivity (Camel and
545 Bermond 1998). Since ozonation plays a more dominant role during
546 plasma treatment with oxygen than with air, this partly explains the
547 decrease in oxidation rate for α -HCH when the feed gas is changed
548 from air to oxygen. Argon plasma consistently performs worse than
549 air plasma. Overall, the observed trends are in good agreement with
550 observations in literature (Hijosa-Valseo et al. 2014). The better
551 performance of O_2 in comparison to air can be explained with
552 different effects:

- 553 • In the absence of nitrogen, less aqueous O_3 and OH
554 scavengers are generated, such as HNO_3 , NO_2^- and NO (see
555 section 3.2.6 for more details).
- 556 • The higher O_2 content leads to higher O_3 production in the
557 plasma chamber.
- 558 • With pure O_2 , aqueous nitrite and nitrate formation is
559 prevented (see section 3.1), resulting in a smaller pH drop
560 and thus a better peroxone performance (Kalra et al. 2011,
561 Lukes et al. 2014).

562

563 **3.2.6. Single-pass experiments**

564

565 Most plasma reactors described in literature operate in batch mode,
566 where the solution under treatment is located inside the reactor
567 during the complete treatment time. Such reactor configurations are,
568 however, unpractical for real-world applications where a large
569 volume needs to be treated in a short time. In this line of thought, it is
570 more attractive to use a reactor in single-pass operation, where water
571 is flowing through the system only once. Therefore, our reactor was
572 modified to work in single-pass mode and micropollutant removal is
573 investigated for three different configurations:

- 574 • a configuration where influent water exclusively flows
575 through the plasma chamber (only plasma);
- 576 • a cascade configuration where influent water first flows
577 through the plasma chamber and subsequently flows through
578 the ozonation chamber (plasma before ozone);
- 579 • a cascade configuration where influent water first flows
580 through the ozonation chamber and subsequently flows
581 through the plasma chamber (ozone before plasma).

582 The latter is illustrated in Figure 6. To allow accurate comparison
583 with the reactor in batch mode, all experiments were conducted with
584 the same standard settings enlisted in Table 1. Before each
585 experiment of the cascade configurations, the ozonation chamber was
586 filled with the initial solution up to the same height of 25.7 cm as
587 used in batch mode. During plasma treatment, samples of the effluent
588 solution were taken after the same treatment times as in the batch

589 mode experiments. All samples were analysed with GC-MS to
590 determine the time-averaged micropollutant concentration in the
591 effluent.

592

593 The removal percentages and corresponding EEO values are given in
594 Table 4. EEO (in kWh/m³) is calculated with the formula introduced
595 by Bolton et al. for reactors in flow-through operation (Bolton et al.
596 1996):

$$597 \quad EEO = \frac{P}{A \times F \times \log(C_0/C_f)} \quad (8.7)$$

598 where P is applied power (in W), A = 3.6 × 10⁶ J/kWh is a unit
599 conversion factor, F is the water flow rate (m³/s) in the flow-through
600 system and C₀ and C_f are the initial and final concentration (in g/L),
601 respectively. For all three flow-through mode configurations,
602 operation without plasma resulted in the same removal percentage
603 and is therefore given as one value. Surprisingly, removal without
604 plasma is most effective for PeCB, while this compound was
605 observed to be the most resistant to adsorption in batch mode (see
606 Figure 3). As PeCB has very high volatility, this apparent
607 contradiction can be explained with air stripping in the plasma
608 chamber.

609

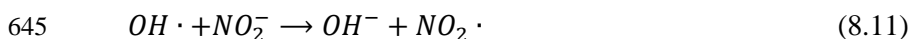
610 Using the hydraulic residence time of 4.20 min and the reaction rate
611 constants from Table 2 for standard settings in batch mode, the
612 corresponding removal percentage in batch mode is calculated, as
613 given in Table 4. According to the resulting removal percentages,
614 single pass mode is performing as good as or better than batch mode
615 for removal of the different compounds.

616

617 In Table 4, comparison of the reactor in absence of the ozonation
618 chamber to the cascade configuration from Figure 6, where plasma
619 gas bubbling precedes treatment in the plasma chamber, clearly
620 shows that energy efficiency approximately doubles when the
621 ozonation chamber is added to the reactor. As should be noted, this
622 cascade configuration performs considerably better for removal of all
623 micropollutants than the reverse cascade configuration. As the most
624 likely reason, this is because of more efficient ozonation of untreated
625 solution as compared to plasma-treated solution. In the plasma
626 chamber, transfer of nitric oxides into the solution leads to the
627 formation of NO_2^- , a known O_3 scavenger through the reaction



629 with reported reaction rate of $k = 1.6 - 5.0 \times 10^5 \text{ M}^{-1}\text{s}^{-1}$ (Damschen
630 and Martin 1983, Garland et al. 1980, Hoigné et al. 1985, Penkett
631 1972). When the solution enters the ozonation chamber afterwards,
632 the aqueous NO_2^- , is mixed rapidly throughout the solution under
633 influence of the bubbling, inhibiting the ozonation process. The
634 transfer of nitric oxides into the solution by the bubbling process in
635 the ozonation chamber is, on the other hand, relatively small, as
636 confirmed by the limited decrease in pH (see Figure 2b). Therefore,
637 ozonation has a stronger effect in the cascade configuration of Figure
638 6 than in the reverse setting. This scavenging mechanism has been
639 reported before in water treatment processes with air plasma (Lukes
640 et al. 2014). Additionally, aqueous OH radicals introduced by means
641 of the bubbled plasma gas can be scavenged as well by reactive
642 nitrogen species through the reactions



646 with reaction rates of $k = 1.0 - 2 \times 10^{10} \text{ M}^{-1}\text{s}^{-1}$ (Seddon et al. 1973,
647 Strehlow and Wagner 1982, Treinin and Hayon 1970), $k = 5.3 - 14 \times$
648 $10^7 \text{ M}^{-1}\text{s}^{-1}$ (Jiang et al. 1992, Katsumura et al. 1991) and $k = 6.0 - 14$
649 $\times 10^5 \text{ M}^{-1}\text{s}^{-1}$ (Adams et al. 1965a, b, Barker et al. 1970, Buxton 1969,
650 Løgager and Sehested 1993, Treinin and Hayon 1970), respectively.
651 The $NO_2 \cdot$ radical formed in Equation 8.11 has a redox potential of
652 1.04 V (Moniczewski et al. 2015, Squadrito and Pryor 2002) and is
653 therefore significantly less reactive than the OH radical reagent with
654 a redox potential of 2.80 V.

655

656 Energy efficiency for micropollutant removal in the cascade
657 configuration of Figure 6 is in the same order of magnitude as in
658 batch mode. As a negative effect, energy efficiency decreases in
659 flow-through mode with $22 \pm 5 \%$ for isoproturon and $15 \pm 6 \%$ for
660 diuron. As a positive effect, energy efficiency increases with 32 ± 10
661 $\%$ for alachlor, $56 \pm 10 \%$ for α -HCH and $96 \pm 16 \%$ for PeCB. Since
662 the most persistent compounds, α -HCH and PeCB, are removed
663 significantly more effectively, while the EEO increase for
664 isoproturon is relatively small, these results speak in favor of the
665 flow-through system for general application. To our knowledge, this
666 is the first time that a comparison in energy efficiency of organic
667 decomposition has been made between batch mode and single-pass
668 mode of the same reactor. These results seem to suggest that EEO
669 values in batch mode are representative for the energy efficiency of

670 an identical reactor in flow-through mode, at least in order of
671 magnitude. Yet, it is uncertain whether this can be generalized for
672 other reactor types as well.

673 4. Conclusion

674 In this work, we have investigated a new type of plasma reactor for
675 water treatment, in which micropollutant decomposition by
676 atmospheric dielectric barrier discharge (DBD) is combined with
677 adsorption on activated carbon textile and with extra bubbling of
678 generated ozone. During treatment in the reactor, solution
679 conductivity gradually rises, while pH drops abruptly in the first
680 minutes of treatment, to slowly decrease further afterwards. Kinetic
681 analysis for the removal of five pesticides led to the following new
682 insights:

- 683 • Energy efficiency for the removal in standard conditions
684 ranges over one order of magnitude, from 3.9 to 26 kWh/m³,
685 with increasing value in the order diuron < isoproturon <
686 alachlor < PeCB < α -HCH. The contribution of evaporation
687 as well as adsorption to the removal process is often
688 significant, but strongly depends on compound properties.
- 689 • As shown for isoproturon, the initial pH has a strong effect
690 on the removal rate, which is explained with a change in
691 oxidation rates of ozonation and the peroxone process.
- 692 • Addition of the salts NaH₂PO₄ and Na₂SO₄ does not
693 influence the removal process, while NaHCO₃, as an OH
694 radical scavenger, lowered the oxidation rate.

- 695 • Investigation of the removal energy efficiency as a function
696 of the initial micropollutant concentration showed a strongly
697 increasing trend of G_{50} and a slight increase in EEO for
698 higher concentrations, in agreement with results from other
699 authors. Energy efficiency displays limited changes and no
700 clear trend under power variation at fixed duty cycle,
701 indicating that removal rate can be increased with little loss
702 in efficiency.
- 703 • Increasing duty cycle, on the other hand, results in
704 remarkably lower energy efficiency. This can be explained
705 with stronger formation of nitrites and nitrates, which are
706 known scavengers of OH radicals or ozone. Also, this can be
707 caused by shorter plasma off time and thus less organic
708 decomposition during the moments without power input or
709 by O_3 and H_2O_2 inhibition due to plasma gas temperature
710 increase.
- 711 • Generally, the oxidation process is enhanced when oxygen is
712 used as feed gas, except for α -HCH, most likely due to its
713 strong resistance to ozonation. Argon, on the other hand,
714 performs worse than air for removal of all compounds.
- 715 • Using the reactor in single-pass mode, where water flows
716 through the treatment chambers only once, enhanced the
717 removal process of the most persistent compounds α -HCH
718 and PeCB, while it performed only slightly worse for diuron
719 and isoproturon removal. Comparison with single pass-mode
720 experiments without the ozonation chamber proves that
721 energy efficiency approximately doubles with the addition of

722 ozonation chamber. Nonetheless, it is important to let the
723 influent water flow through the ozonation chamber first and
724 only afterwards through the plasma chamber, since the
725 reverse cascade configuration gives consistently worse
726 energy efficiency. This is explained with scavenging of
727 ozone by NO_2^- ions, which are introduced into the solution
728 during direct plasma contact in the plasma chamber.

729 **Acknowledgements**

730 The authors would like to thank Carbon Cloth Division for Zorflex[®]
731 samples and personally thank Jack Taylor for fruitful discussion of
732 active carbon water treatment processes.

733 **References**

- 734 Adams, G., Boag, J. and Michael, B. (1965a) Reactions of the hydroxyl
735 radical. Part 2.—Determination of absolute rate constants. Transactions of
736 the Faraday Society 61, 1417-1424.
- 737 Adams, G., Boag, J. and Michael, B. (1965b) Spectroscopic studies of
738 reactions of the OH radical in aqueous solutions. Reaction of OH with the
739 ferrocyanide ion. Transactions of the Faraday Society 61, 492-505.
- 740 Barker, G., Fowles, P. and Stringer, B. (1970) Pulse radiolytic induced
741 transient electrical conductance in liquid solutions. Part 2.—Radiolysis of
742 aqueous solutions of NO_3^- , NO_2^- and $\text{Fe}(\text{CN})_6^{3-}$. Transactions of the
743 Faraday Society 66, 1509-1519.
- 744 Bolton, J.R., Bircher, K.G., Tumas, W. and Tolman, C.A. (1996) Figures-of
745 merit for the technical development and application of advanced oxidation
746 processes. Journal of Advanced Oxidation Technologies 1, 13-17.
- 747 Buxton, G. (1969) Pulse radiolysis of aqueous solutions. Some rates of

- 748 reaction of OH and O₂-and pH dependence of the Yield of O₃-3.
749 Transactions of the Faraday Society 65, 2150-2158.
- 750 Camel, V. and Bermond, A. (1998) The use of ozone and associated
751 oxidation processes in drinking water treatment. Water Research 32(11),
752 3208-3222.
- 753 Catalkaya, E.C. and Kargi, F. (2009) Dehalogenation, degradation and
754 mineralization of diuron by peroxone (peroxide/ozone) treatment. Journal of
755 Environmental Science and Health, Part A 44(6), 630-638.
- 756 Cater, S.R., Stefan, M.I., Bolton, J.R. and Safarzadeh-Amiri, A. (2000)
757 UV/H₂O₂ treatment of methyl tert-butyl ether in contaminated waters.
758 Environmental Science & Technology 34(4), 659-662.
- 759 Damschen, D.E. and Martin, L.R. (1983) Aqueous aerosol oxidation of
760 nitrous acid by O₂, O₃ and H₂O₂. Atmospheric Environment (1967)
761 17(10), 2005-2011.
- 762 EC (2006) Directive 2006/118/EC of the European Parliament and of the
763 Council of 12 December 2006 on the protection of groundwater against
764 pollution and deterioration, p. 26.
- 765 EPA, U.S. (2007) Atrazine, Toxicity and Exposure Assessment for
766 Children's Health (TEACH), Chemical Summaries, p. 6.
- 767 Eriksson, M. (2005) Ozone chemistry in aqueous solution: ozone
768 decomposition and stabilisation, Royal Institute of Technology, Stockholm,
769 Sweden.
- 770 Fouodjouo, M., Laminsi, S., Djepang, S.A., Tadam, D. and Brisset, J.-L.
771 (2013) Non-Thermal Plasma Coupled to TiO₂ Applicable for the Removal
772 of Paraquat from Aqueous Solutions. International Journal of Research in
773 Chemistry and Environment 3(1), 316-326.
- 774 Gao, L., Sun, L., Wan, S., Yu, Z. and Li, M. (2013) Degradation kinetics
775 and mechanism of emerging contaminants in water by dielectric barrier
776 discharge non-thermal plasma: The case of 17 β -Estradiol. Chemical
777 Engineering Journal 228, 790-798.

- 778 Garland, J.A., Elzerman, A.W. and Penkett, S.A. (1980) The mechanism for
779 dry deposition of ozone to seawater surfaces. *Journal of Geophysical*
780 *Research: Oceans* 85(C12), 7488-7492.
- 781 Ghatak, H.R. (2014) Advanced oxidation processes for the treatment of
782 biorecalcitrant organics in wastewater. *Critical Reviews in Environmental*
783 *Science and Technology* 44(11), 1167-1219.
- 784 Ghodbane, H., Nikiforov, A.Y., Hamdaoui, O., Surmont, P., Lynen, F.,
785 Willems, G. and Leys, C. (2014) Non-thermal Plasma Degradation of
786 Anthraquinonic Dye in Water: Oxidation Pathways and Effect of Natural
787 Matrices. *Journal of Advanced Oxidation Technologies* 17(2), 372-384.
- 788 Giacomazzi, S. and Cochet, N. (2004) Environmental impact of diuron
789 transformation: a review. *Chemosphere* 56(11), 1021-1032.
- 790 Haag, W.R. and Yao, C.D. (1992) Rate constants for reaction of hydroxyl
791 radicals with several drinking water contaminants. *Environmental Science*
792 *& Technology* 26(5), 1005-1013.
- 793 Heidt, L.J. and Landi, V.R. (1967) Stabilization of ozone, United States
794 Patent Office, 3,352,642.
- 795 Hijosa-Valsero, M., Molina, R., Montràs, A., Müller, M. and Bayona, J.M.
796 (2014) Decontamination of waterborne chemical pollutants by using
797 atmospheric pressure nonthermal plasma: a review. *Environmental*
798 *Technology Reviews* 3(1), 71-91.
- 799 Hijosa-Valsero, M., Molina, R., Schikora, H., Müller, M. and Bayona, J.M.
800 (2013) Removal of priority pollutants from water by means of dielectric
801 barrier discharge atmospheric plasma. *Journal of Hazardous Materials* 262,
802 664-673.
- 803 Hoigné, J., Bader, H., Haag, W. and Staehelin, J. (1985) Rate constants of
804 reactions of ozone with organic and inorganic compounds in water—III.
805 Inorganic compounds and radicals. *Water Research* 19(8), 993-1004.
- 806 Jiang, P.Y., Katsumura, Y., Ishigure, K. and Yoshida, Y. (1992) Reduction
807 potential of the nitrate radical in aqueous solution. *Inorganic Chemistry*

- 808 31(24), 5135-5136.
- 809 Kalra, S.S., Mohan, S., Sinha, A. and Singh, G. (2011) Advanced oxidation
810 processes for treatment of textile and dye wastewater: a review, pp. 271-
811 275, IACSIT Press Singapore.
- 812 Katsumura, Y., Jiang, P., Nagaishi, R., Oishi, T., Ishigure, K. and Yoshida,
813 Y. (1991) Pulse radiolysis study of aqueous nitric acid solutions: formation
814 mechanism, yield, and reactivity of NO₃ radical. *The Journal of Physical*
815 *Chemistry* 95(11), 4435-4439.
- 816 Løgager, T. and Sehested, K. (1993) Formation and decay of peroxyxynitrous
817 acid: a pulse radiolysis study. *The Journal of Physical Chemistry* 97(25),
818 6664-6669.
- 819 Lukes, P., Dolezalova, E., Sisrova, I. and Clupek, M. (2014) Aqueous-phase
820 chemistry and bactericidal effects from an air discharge plasma in contact
821 with water: evidence for the formation of peroxyxynitrite through a pseudo-
822 second-order post-discharge reaction of H₂O₂ and HNO₂. *Plasma Sources*
823 *Science and Technology* 23(1), 015019.
- 824 Luo, Y., Guo, W., Ngo, H.H., Nghiem, L.D., Hai, F.I., Zhang, J., Liang, S.
825 and Wang, X.C. (2014) A review on the occurrence of micropollutants in
826 the aquatic environment and their fate and removal during wastewater
827 treatment. *Science of The Total Environment* 473-474, 619-641.
- 828 Magureanu, M., Piroi, D., Mandache, N.B., David, V., Medvedovici, A. and
829 Parvulescu, V.I. (2010) Degradation of pharmaceutical compound
830 pentoxifylline in water by non-thermal plasma treatment. *Water Research*
831 44(11), 3445-3453.
- 832 McDonogh, C.F. and Sanders, N.J. (1995) Peroxymonosulfuric acid formed
833 by reaction of hydrogen peroxide and sulfuric acid, United States Patents,
834 US005429812A.
- 835 Milla, S., Depiereux, S. and Kestemont, P. (2011) The effects of estrogenic
836 and androgenic endocrine disruptors on the immune system of fish: a
837 review. *Ecotoxicology* 20(2), 305-319.

- 838 Moniczewski, A., Gawlik, M., Smaga, I., Niedzielska, E., Krzek, J.,
839 Przegaliński, E., Pera, J. and Filip, M. (2015) Oxidative stress as an
840 etiological factor and a potential treatment target of psychiatric disorders.
841 Part 1. Chemical aspects and biological sources of oxidative stress in the
842 brain. *Pharmacological Reports* 67(3), 560-568.
- 843 Moreno-Castilla, C. (2004) Adsorption of organic molecules from aqueous
844 solutions on carbon materials. *Carbon* 42(1), 83-94.
- 845 Nakagawa, Y., Mitamura, S., Fujiwara, Y. and Nishitani, T. (2003)
846 Decolorization of Rhodamine B in Water by Pulsed High-Voltage Gas
847 Discharge. *Japanese Journal of Applied Physics* 42(Part 1, No. 3), 1422-
848 1428.
- 849 Ognier, S., Iya-sou, D., Fourmond, C. and Cavadias, S. (2009) Analysis of
850 Mechanisms at the Plasma–Liquid Interface in a Gas–Liquid Discharge
851 Reactor Used for Treatment of Polluted Water. *Plasma Chemistry and
852 Plasma Processing* 29(4), 261-273.
- 853 Olszewski, P., Li, J., Liu, D. and Walsh, J. (2014) Optimizing the electrical
854 excitation of an atmospheric pressure plasma advanced oxidation process.
855 *Journal of Hazardous Materials* 279, 60-66.
- 856 Oturan, M.A. and Aaron, J.-J. (2014) Advanced oxidation processes in
857 water/wastewater treatment: principles and applications. A review. *Critical
858 Reviews in Environmental Science and Technology* 44(23), 2577-2641.
- 859 Penkett, S. (1972) Oxidation of SO₂ and other atmospheric gases by ozone
860 in aqueous solution. *Nature* 240(101), 105-106.
- 861 Rizzo, L., Manaia, C., Merlin, C., Schwartz, T., Dagot, C., Ploy, M.,
862 Michael, I. and Fatta-Kassinos, D. (2013) Urban wastewater treatment
863 plants as hotspots for antibiotic resistant bacteria and genes spread into the
864 environment: a review. *Science of The Total Environment* 447, 345-360.
- 865 Roche, P. and Prados, M. (1995) Removal of pesticides by use of ozone or
866 hydrogen peroxide/ozone. *Ozone: Science & Engineering* 17(6), 657-672.
- 867 Seddon, W., Fletcher, J. and Sopchyshyn, F. (1973) Pulse radiolysis of nitric

- 868 oxide in aqueous solution. *Canadian Journal of Chemistry* 51(7), 1123-1130.
- 869 Spivey, J., Han, Y. and Dooley, K. (2015) *Catalysis, Volume 27 of*
- 870 *Specialist Periodical Reports*, Royal Society of Chemistry, ISBN
- 871 9781782620549.
- 872 Squadrito, G.L. and Pryor, W.A. (2002) Mapping the reaction of
- 873 peroxyxynitrite with CO₂: energetics, reactive species, and biological
- 874 implications. *Chemical research in toxicology* 15(7), 885-895.
- 875 Strehlow, H. and Wagner, I. (1982) Flash photolysis in aqueous nitrite
- 876 solutions. *Zeitschrift für Physikalische Chemie* 132(2), 151-160.
- 877 Treinin, A. and Hayon, E. (1970) Absorption spectra and reaction kinetics
- 878 of NO₂, N₂O₃, and N₂O₄ in aqueous solution. *Journal of the American*
- 879 *Chemical Society* 92(20), 5821-5828.
- 880 Vanraes, P., Willems, G., Daels, N., Van Hulle, S.W., De Clerck, K.,
- 881 Surmont, P., Lynen, F., Vandamme, J., Van Durme, J. and Nikiforov, A.
- 882 (2015a) Decomposition of atrazine traces in water by combination of non-
- 883 thermal electrical discharge and adsorption on nanofiber membrane. *Water*
- 884 *Research* 72, 361-371.
- 885 Vanraes, P., Willems, G., Nikiforov, A., Surmont, P., Lynen, F.,
- 886 Vandamme, J., Van Durme, J., Verheust, Y.P., Van Hulle, S.W.H.,
- 887 Dumoulin, A. and Leys, C. (2015b) Removal of atrazine in water by
- 888 combination of activated carbon and dielectric barrier discharge. *Journal of*
- 889 *Hazardous Materials* 299, 647-655.
- 890 Verlicchi, P., Galletti, A., Petrovic, M. and Barceló, D. (2010) Hospital
- 891 effluents as a source of emerging pollutants: an overview of micropollutants
- 892 and sustainable treatment options. *Journal of Hydrology* 389(3), 416-428.
- 893 WHO (2008) World Health Organisation, Guidelines for drinking-water
- 894 quality: recommendations, World Health Organization.
- 895 Wohlers, J., Koh, I.-O., Thiemann, W. and Rotard, W. (2009) Application of
- 896 an air ionization device using an atmospheric pressure corona discharge
- 897 process for water purification. *Water, Air, and Soil Pollution* 196(1-4), 101-

898 113.

899 Yao, C.D. and Haag, W.R. (1991) Rate constants for direct reactions of

900 ozone with several drinking water contaminants. Water Research 25(7),

901 761-773.

ACCEPTED MANUSCRIPT

Figure 1. Structural formulas of the pesticides used in this work.

Figure 2. Measured pH and conductivity data during experiments with reactor settings as specified in Table 1. Initial conductivity was set at 350 $\mu\text{S}/\text{cm}$ by addition of $\text{NaH}_2\text{PO}_4 \cdot 2\text{H}_2\text{O}$ to demineralized water. (a) and (b) pH and conductivity as a function of treatment time for applied power of 59 W. In (b), pH evolution is compared with an experiment where the solution is subjected to plasma gas bubbling alone. In the latter configuration, the investigated solution was not in direct contact with the active plasma zone, but another solution was recirculated through the plasma chamber in an isolated circuit. (c) and (d) pH and conductivity after 30 min treatment time for different duty cycles.

Figure 3. Removal kinetics for the 5 micropollutants in the reactor without plasma generation and in absence of Zorflex, but with air bubbling (only evaporation), without plasma generation, but with Zorflex and air bubbling (evaporation + adsorption) and with plasma generation in the standard settings (plasma + O_3). The full lines represent the best exponential fit.

Figure 4. Removal kinetics in the reactor with standard settings for different duty cycles.

Figure 5. Removal kinetics in the reactor with standard settings for different feed gases.

Figure 6. Cascade configuration of the reactor in single-pass mode where influent water first enters the ozonation chamber and subsequently passes through the plasma chamber.

ACCEPTED MANUSCRIPT

Table 1. Reactor standard settings for the experiments in this work.

Experimental parameter	Value/description
Voltage amplitude	7.9-8.4 kV
Input power	See Table 3
AC frequency	47.8 kHz
Modulation frequency	33.3 Hz
Duty cycle	15.0%
Treated volume	500 mL
Water flow rate	95.3 mL/min
Gas flow rate	1.00 SLM
Feed gas	air
Inter-electrode distance	2.25 mm

Table 2. Initial concentration C_0 , applied power, reciprocal of the time constant τ_e for only evaporation, reciprocal of the time constant τ_{e+a} for evaporation and adsorption, reaction rate k , energy yield G_{50} and electrical energy per order EEO for the reactor in standard settings.

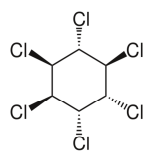
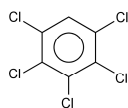
	α -HCH	PeCB	alachlor	diuron	isoproturon
C_0 ($\mu\text{g/L}$)	215 ± 6	67 ± 2	57 ± 4	114 ± 6	101 ± 3
Power (W)	49.9 ± 1.8	48.9 ± 1.7	40.3 ± 0.3	39.7 ± 0.5	41.0 ± 1.0
$1/\tau_e$ (10^{-5} s^{-1})	76 ± 3	314 ± 17	23 ± 3	49 ± 6	1.3 ± 1.5
$1/\tau_{e+a}$ (10^{-4} s^{-1})	17.9 ± 1.2	35 ± 3	17 ± 2	17 ± 3	11.0 ± 1.0
k (10^{-3} s^{-1})	2.45 ± 0.14	5.1 ± 0.3	8.5 ± 0.4	13.0 ± 0.2	10.3 ± 0.4
G_{50} (mg/kWh)	13.7 ± 1.0	9.0 ± 0.6	15.5 ± 1.3	49 ± 3	33.0 ± 1.8
EEO (kWh/m^3)	26.1 ± 1.7	12.2 ± 0.7	6.1 ± 0.3	3.90 ± 0.09	5.1 ± 0.2

Table 3. Energy yield G_{50} and electrical energy per order EEO for the reactor in standard settings for different feed gases.

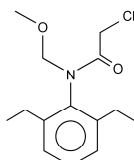
		α -HCH	PeCB	alachlor	diuron	isoproturon
G_{50} (mg/kWh)	air	13.7 ± 1.0	9.0 ± 0.6	15.5 ± 1.3	49 ± 3	33.0 ± 1.8
G_{50} (mg/kWh)	Ar	14.2 ± 0.6	6.8 ± 0.4	13.8 ± 1.3	30 ± 2	5.6 ± 0.7
G_{50} (mg/kWh)	O ₂	8.0 ± 0.4	34.3 ± 1.3	56 ± 8	114 ± 10	
EEO (kWh/m^3)	air	26.1 ± 1.7	12.2 ± 0.7	6.1 ± 0.3	3.90 ± 0.09	5.1 ± 0.2
EEO (kWh/m^3)	Ar	25.1 ± 0.7	16.2 ± 0.8	6.9 ± 0.4	6.3 ± 0.3	30 ± 3
EEO (kWh/m^3)	O ₂	44 ± 2	3.22 ± 0.08	1.7 ± 0.2	1.67 ± 0.12	

Table 4. Removal percentage and electrical energy per order EEO for the reactor in single-pass mode for the different configurations. In the “no plasma” experiments, neither plasma nor ozone was used. For comparison, also the removal percentage at the hydraulic retention time 4.20 min and the EEO value in batch mode are given, for the same standard settings.

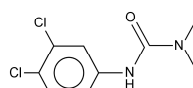
		α -HCH	PeCB	alachlor	diuron	isoproturon
removal (%)	no plasma	31.7 ± 1.2	75.7 ± 0.6	44.6 ± 0.5	60.9 ± 0.9	37.6 ± 1.4
	only plasma	43.7 ± 1.5	79.0 ± 0.7	75.1 ± 0.4	79.3 ± 0.5	
	plasma before ozone	59 ± 2	82.6 ± 0.7	87 ± 2	90.5 ± 1.3	75.9 ± 0.4
	ozone before plasma	64.8 ± 1.0	94.5 ± 0.6	97.0 ± 0.6	96.9 ± 0.7	91.6 ± 1.0
	batch mode (4.20 min)	46.1 ± 1.9	72 ± 2	88.3 ± 1.2	96.2 ± 0.2	92.5 ± 0.8
EEO (kWh/m^3)	only plasma	30.1 ± 1.5	11.4 ± 0.3	11.6 ± 0.2	9.9 ± 0.2	
	plasma before ozone	18.4 ± 1.1	9.9 ± 0.4	8.0 ± 0.7	6.7 ± 0.4	11.5 ± 0.3
	ozone before plasma	16.7 ± 0.7	6.2 ± 0.3	4.6 ± 0.3	4.6 ± 0.3	6.5 ± 0.3
	batch mode (4.20 min)	26.1 ± 1.7	12.2 ± 0.8	6.1 ± 0.3	3.90 ± 0.09	5.1 ± 0.2

 α -HCH

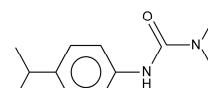
PeCB



alachlor

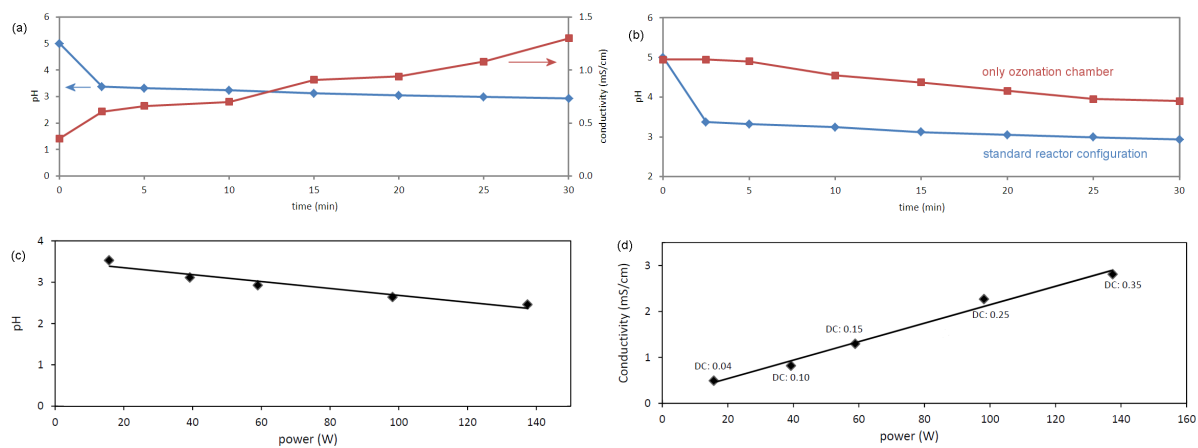


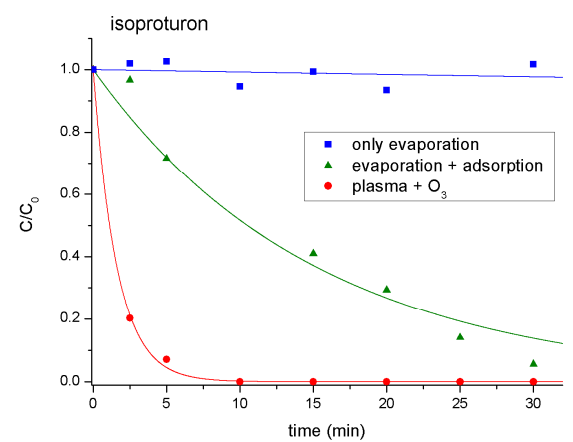
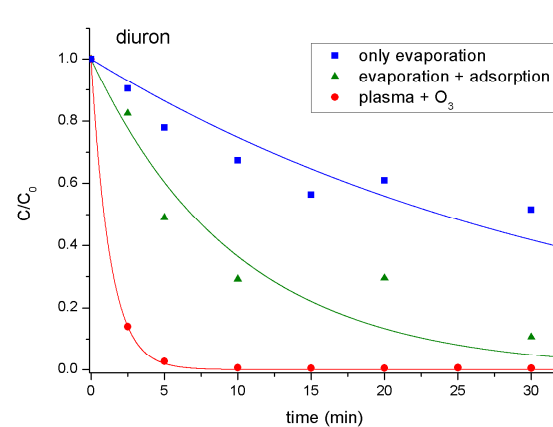
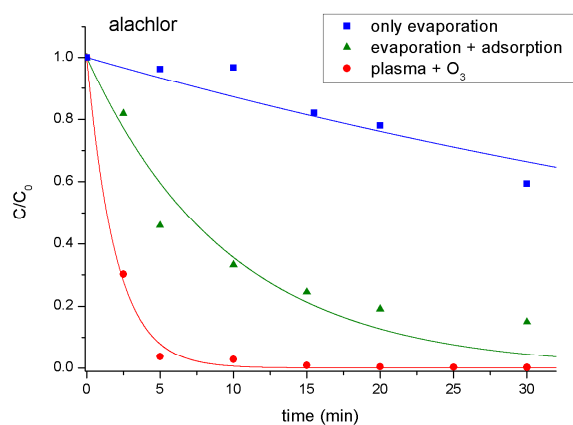
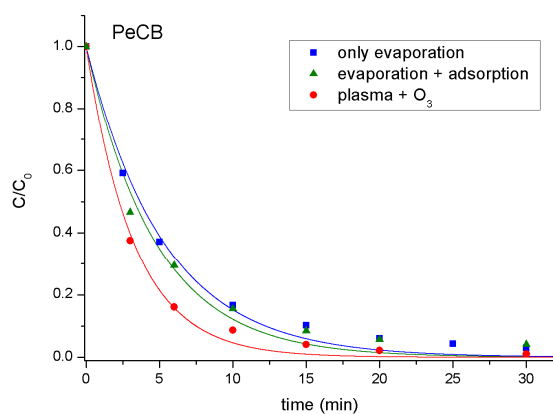
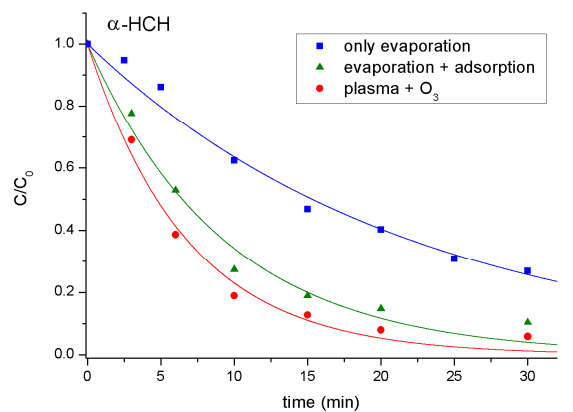
diuron

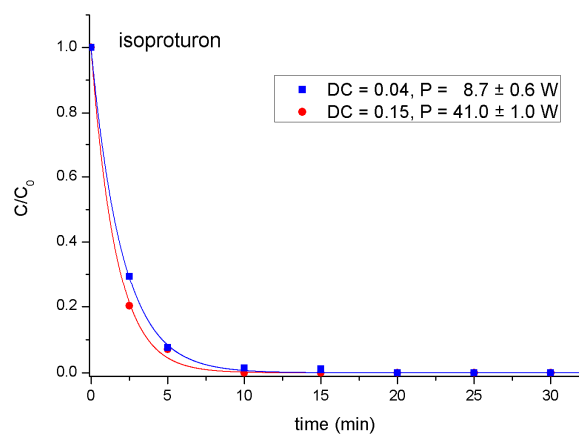
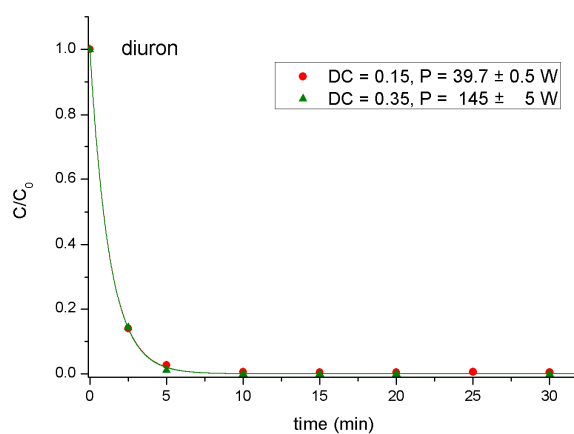
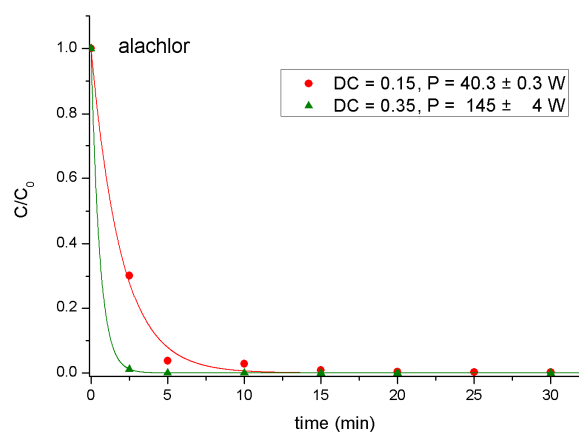
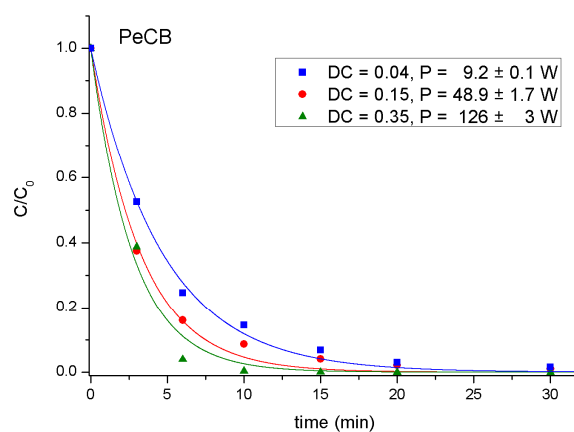
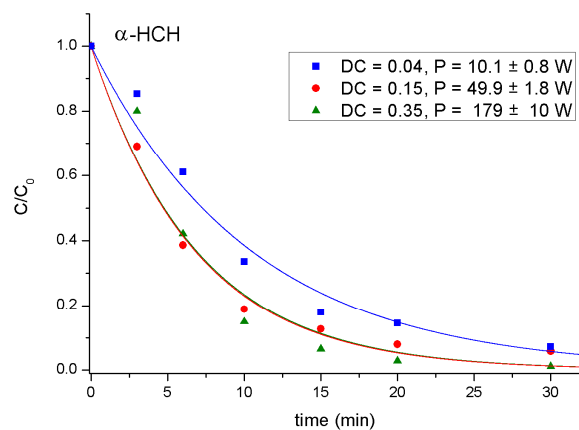


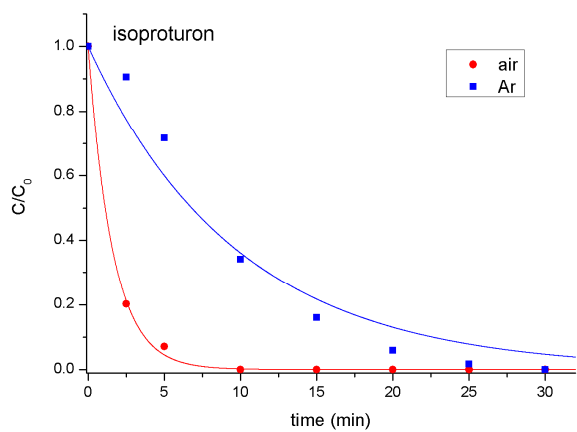
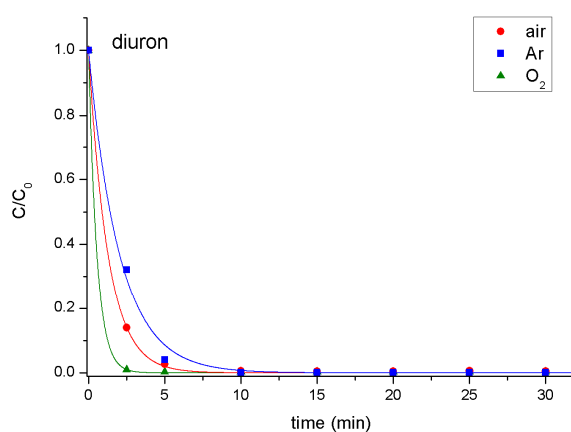
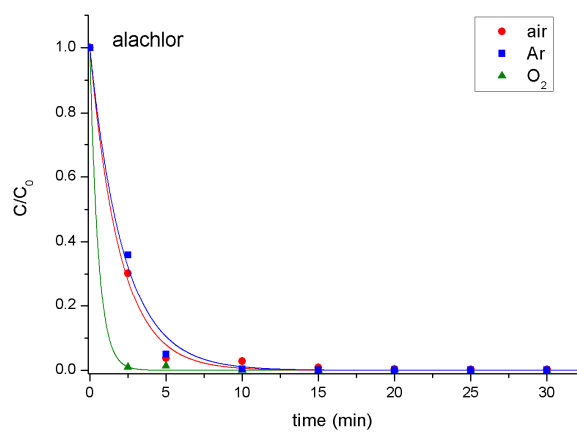
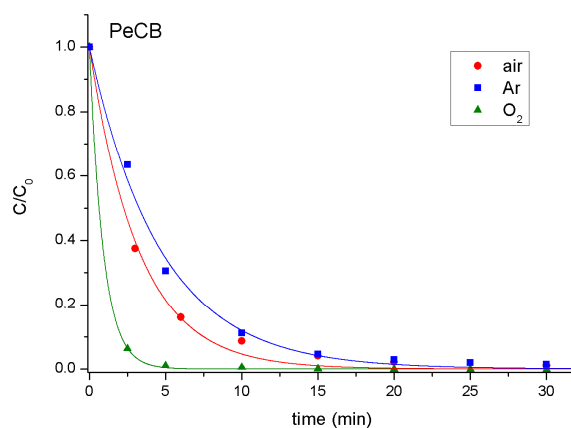
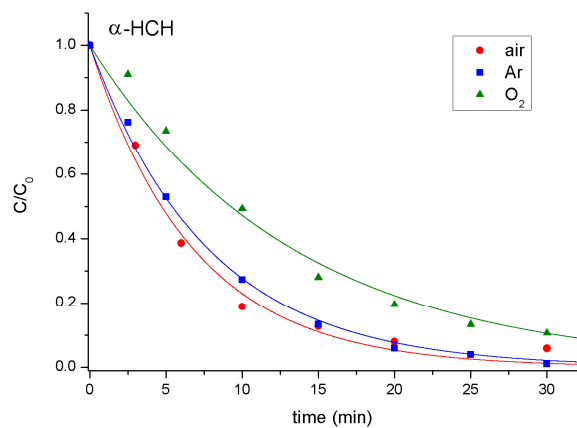
isoproturon

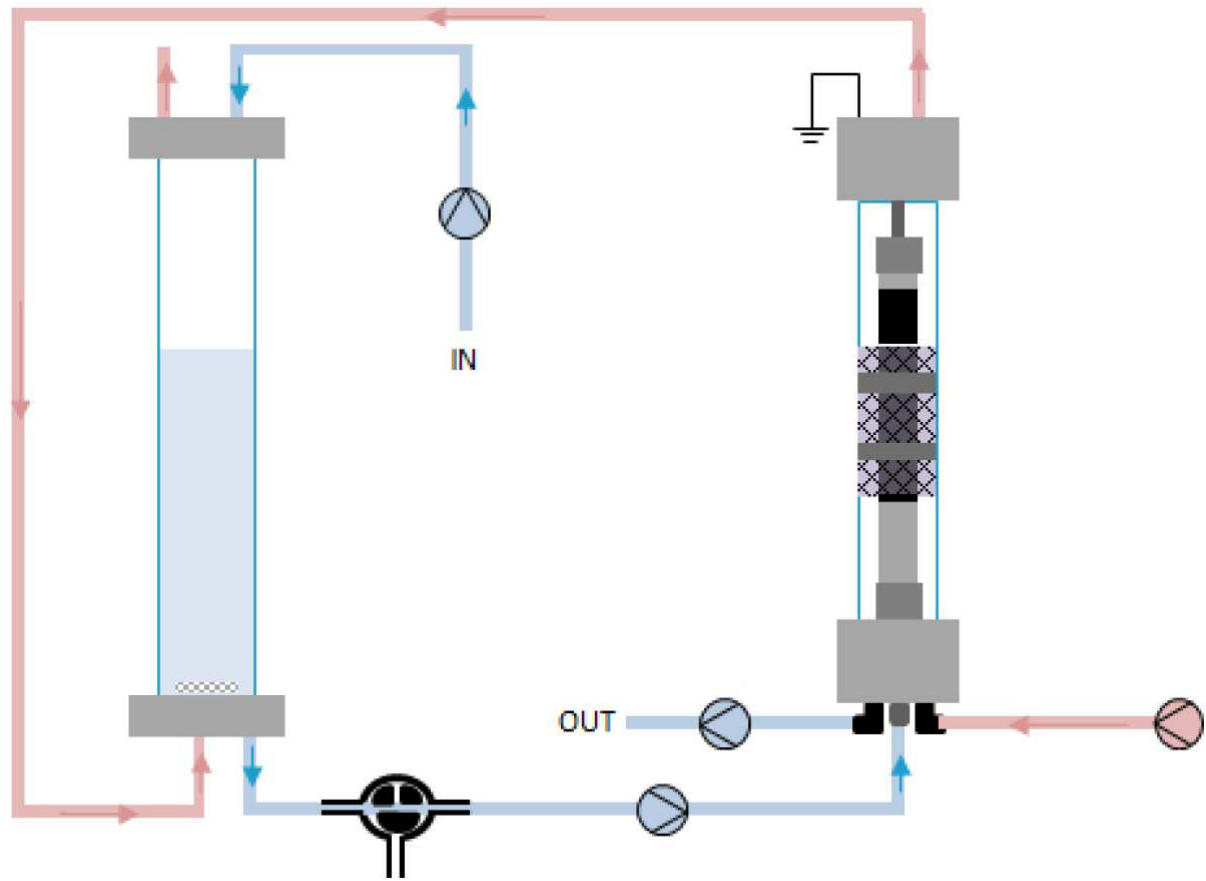
ACCEPTED MANUSCRIPT











Highlights

- A novel dielectric barrier discharge reactor is investigated for pollutant removal.
- Five persistent pesticides are used in low concentrations around 100 µg/L.
- Removal efficiency increases for decreasing duty cycle and pesticide concentration.
- Oxygen plasma is more effective than air and argon plasma.
- The reactor in single-pass operation performs better than in recirculating mode.